Coupled Systems Mechanics, *Vol. 6, No. 1 (2017) 1-15*
DOI: https://doi.org/10.12989/csm.2017.6.1.001

Influence of the microstructure on effective mechanical properties of carbon nanotube composites

Sven Drücker[*1], Jana Wilmers[2a] and Swantje Bargmann[2b]

[1]*Institute of Polymer Composites, Hamburg University of Technology, Denickestr. 15, 21073 Hamburg, Germany*
[2]*Chair of Solid Mechanics, University of Wuppertal, Gaussstr. 20, 42119 Wuppertal, Germany*

(Received November 10, 2016, Revised March 15, 2017, Accepted April 5, 2017)

Abstract. Despite the exceptional mechanical properties of individual carbon nanotubes (CNTs), the effective properties of CNT-reinforced composites remain below expectations. The composite's microstructure has been identified as a key factor in explaining this discrepancy. In this contribution, a method for generating representative volume elements of aligned CNT sheets is presented. The model captures material characteristics such as random waviness and entanglement of individual nanotubes. Thus it allows studying microstructural effects on the composite's effective properties.

Simulations investigating the strengthening effect of the application of a pre-stretch on the CNTs are carried out and found to be in very good agreement with experimental values. They highlight the importance of the nanotube's waviness and entanglement for the mechanical behavior of the composite. The presented representative volume elements are the first to accurately capture the waviness and entanglement of CNT sheets for realistically high volume fractions.

Keywords: carbon nanotubes; CNT reinforced composites; RVE generation; representative volume element

1. Introduction

Since their discovery by Iijima (1991) in the 1990s, carbon nanotubes (CNTs) have attracted great interest and have been subject to many studies. Experiments revealed an exceptionally high stiffness (Wong *et al.* 1997, Salvetat *et al.* 1999) and strength (Yu *et al.* 2000, Demczyk *et al.* 2002) of CNTs as well as the ability to withstand large deformations (Demczyk *et al.* 2002, Thostenson *et al.* 2005). Their outstanding mechanical properties raise the desire to employ CNTs in structural components. Especially, the application in composites is promising. Here, a polymer matrix connects individual CNTs and prevents slippage. However, effective mechanical properties reached in CNT composites are far below expectations from rule of mixtures (Goh *et al.* 2014).

∗Corresponding author, Ph.D. Student, E-mail: sven.druecker@tuhh.de
[a]Ph.D., E-mail: wilmers@uni-wuppertal.de
[b]Professor, E-mail: bargmann@uni-wuppertal.de

http://www.techno-press.org/?journal=csm&subpage=8 ISSN: 2234-2184 (Print), 2234-2192 (Online)

Besides other factors such as CNT orientation (Mecklenburg *et al.* 2015) and agglomeration (Goh *et al.* 2014) or interfacial load transfer (Andrews and Weisenberger 2004), the CNT's waviness seems to be a key factor that limits full exploitation of the amazing mechanical properties of CNTs in a composite (Fisher *et al.* 2002 and 2003, Shady *et al.* 2010, Dastgerdi *et al.* 2013).

In order to reduce the waviness and, thus, improve the composite's properties, Nam *et al.* (2014) propose to pre-stretch horizontally aligned CNT sheets before they are incorporated in the polymer matrix in order to reduce the waviness. In an experimental study, they conducted tensile tests after embedding pre-stretched CNT sheets in an epoxy matrix to determine effective mechanical properties of the composite. They observed an increase of more than 80 % in elastic modulus and 110 % in tensile strength after pre-stretching of CNT sheets. As an additional positive side effect of pre-stretching, an increase in volume fraction was detected. This experimental study motivates the present contribution. Here, the effect of pre-stretching the CNT sheets and the influence of the microstructural geometry before the incorporation in a matrix is modelled and investigated numerically with the finite element method.

To date, CNTs are mainly modelled on the atomic scale and often analytical homogenisation techniques are used to determine effective material properties of composites. In *ab-initio* (Hernandez *et al.* 1998, Van Lier *et al.* 2000), molecular dynamics (Yakobson and Smalley 1996, Jin and Yuan 2003) and molecular structural mechanics (Li and Chou 2003, Cheng *et al.* 2009, Wernik *et al.* 2010) simulations, only small sections of individual CNTs are modelled. Analytical homogenisation schemes like Mori-Tanaka were employed to determine the mechanical properties of macroscopic composites, e.g., by Shady *et al.* (2010), Dastgerdi *et al.* (2013) and Tsuda *et al.* (2014). Despite the evident interest in CNT reinforced composites, there is a lack of studies attempting to accurately model the microstructure of a composite with several CNTs and a polymer matrix. As the CNTs' waviness is a dominant factor in the deviation of the composite's properties from expectations, a number of approaches taking into account the waviness have been proposed. Most studies modelled individual CNTs as having a sinusoidal (Fisher *et al.* 2002 and 2003, Bradshaw *et al.* 2003, Paunikar and Kuma 2014) or helical (Shi *et al.* 2004, Shady *et al.* 2010) shapes. However, Ginga *et al.* (2014) point out that the waviness is highly random and regular geometries might not represent it correctly. Subsequently, they extracted points from micrographs of CNTs and used Fourier series or splines to connect these points and recreate single CNTs. Recent studies by Herasati and Zhang (2014) and Stein *et al.* (2015) identify distributions of parameters to describe the waviness from micrographs and utilise them to create CNTs with random waviness.

In the following, an enhanced version of the approach of Herasati and Zhang (2014) is presented in which the randomly generated points are connected by cubic splines to model realistically smooth CNTs without kinks. With these CNT geometries, periodical representative volume elements (RVEs) (Kouznetsova *et al.* 2010, Schneider *et al.* 2016) are built in which an entanglement of randomly wavy CNTs is possible. Numerical studies are carried out to analyse the influences of wavy geometry and pre-stretching on the effective elastic modulus of CNT reinforced composites.

2. RVE generation of the microstructure

To accurately describe the complex microstructure of an aligned CNT sheet, we model

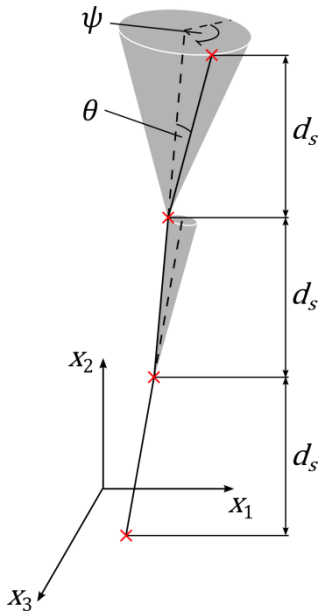

Fig. 1 Stepping scheme to generate spline points for a random wavy CNT. The procedure follows Herasati and Zhang (2014)

individual CNTs based on cubic splines that capture the random waviness of a real CNT. The spline points are randomly generated, using an algorithm based on the approach of Herasati and Zhang (2014). Each CNT is composed of a sequence of straight line segments. Starting from an initial point on the RVE face, each segment is constructed on the basis of a right circular cone where the tip is located at the endpoint of the last segment and the middle axis is in direction of the last segment.

This algorithm is used to generate the geometry defining spline points. At the beginning of the CNT generation procedure, the diameter and the starting point on the bottom surface of the RVE are fixed. Then, new points are generated stepwise until the desired CNT length is reached. To ensure random waviness of the CNT, the angle of the cone θ is randomly assigned based on a normal distribution obtained from analysis of CNT sheet micrographs[†]. The rotational angle ψ describes the position of the point on the cone base and is assigned fully randomly. In contrast to the work of Herasati and Zhang (2014), we set the projected length of each segment in alignment direction to a value d_s. This guarantees that each CNT is constructed with the same amount of points which simplifies the enforcement of periodicity.

After each such generation of a point, the minimum distance to other CNTs is calculated to check for intersections. The determination of the minimum distance is not trivial as the CNTs are

[†]As the simulations are based on the experiments of Nam *et al*. (2014) with CVD synthesized CNTs (Inoue *et al*. 2008), the characteristics of the modelled CNTs are taken from publications of that group. To extract information from the micrographs for the waviness, points are placed along a number of CNTs. The points are connected by line segments and the angle θ between consecutive line segments is calculated for a total of 379 line segments.

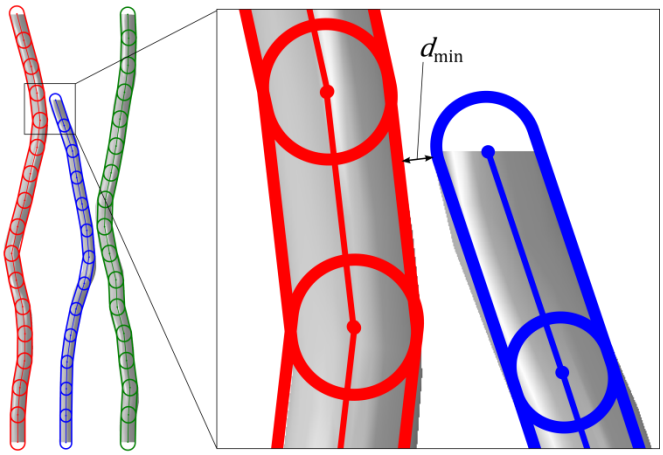

Fig. 2 Discretisation of CNTs into capsules for minimum distance calculation to check for intersections

modelled as cylinders swept along splines. Here, the CNTs are discretised into capsules and the minimum distance towards the capsules of previously generated CNTs is calculated. This discretisation and the basic principle of the minimum distance calculation are illustrated in Fig. 2. If no intersection occurs, the newly generated point is saved. Otherwise, the point is rejected and a new one is generated. In this fashion, new CNTs are generated until the desired volume fraction is reached.

The so established points of an individual CNT are connected using cubic splines instead of the straight line segments employed by Herasati and Zhang (2014). This guarantees C^2 continuity of the modelled CNTs within the RVE and, therefore, prevents artificial kinks and sharp edges in the geometry that might result in unphysical stress concentrations. Furthermore, the procedure as presented by Herasati and Zhang (2014) does not yield a periodic RVE as a CNT entering the RVE at the bottom does not necessarily leave it at the top, resulting in clipped, very short CNTs. To overcome this drawback[‡], we enforce local periodicity by incrementally orienting randomly generated segments close to the RVE's top surface towards the desired end point. In order to guarantee the periodicity of the CNTs, any CNT entering the RVE must leave it at the same point on the opposite side. This is enforced by a linear combination of the randomly generated step vector and a vector pointing in the direction of the desired end point over the last quarter of points with increasing weight on the vector in the direction of the desired end point. Therefore, CNTs are regarded as endless fibres - a reasonable approximation as CNTs have an exceptionally high aspect ratio of 100000 (length/radius).

Based on splines, CNTs are modelled as thin-walled hollow tubes. To this end, a circle with diameter D of a CNT is swept along the spline. This diameter is assigned randomly based on the properties of real CNT sheets, compare Section 4. These CNTs are then discretised with quadrilateral shell elements of type S4R. Reduced integration is used to decrease computational cost.

For the thickness t of the shell elements, the product of the number of walls n_w in a multi-wall

[‡]Instead of a periodic RVE, another option would be to use approximate periodic boundary conditions (Yuan and Fish 2008, Kassem 2010, Schneider *et al.* 2017)

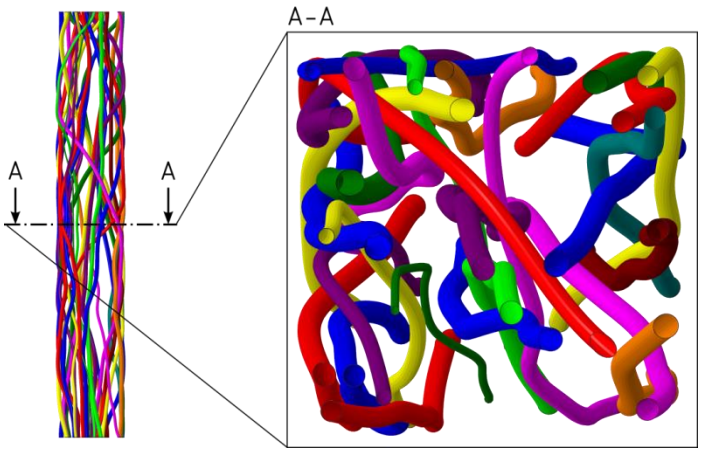

Fig. 3 Cut through CNT sheet RVE illustrating random waviness and entanglement of CNTs

CNT with the thickness of a single CNT wall is used as proposed by Govindjee and Sackmann (1999). For the thickness of a single CNT wall, a value of 0.34 nm is usually assumed corresponding to the inter-wall spacing of CNTs (Grady 2011).

This RVE generation technique captures random waviness and especially entanglement of aligned CNT sheets as visible in Fig. 3. In contrast to previous works on wavy and entangled RVEs (Herasati and Zhang 2014), our RVEs are periodic and allow to study high CNT volume fractions.

3. Modelling pre-stretched CNT composites

As in the experimental procedure proposed by Nam *et al*. (2014), the modelling of pre-stretched CNT composites is a two-step procedure. In a first simulation, the RVE of the CNT sheet is stretched using tensile loading in alignment direction. This deformed and pre-stressed CNT sheet is then embedded into a polymer matrix. In the following, the underlying principles of the two simulation steps are described. Numerical studies using these principles are then presented in Section 4.

3.1 Application of the pre-stretch

For pre-stretching the CNT sheet, all displacement degrees of freedom are fixed at the bottom. At the top, displacements in transverse directions are fixed while a displacement u_{ps} corresponding to the desired pre-stretch is applied in alignment direction. The theory of finite deformations is used since geometric nonlinearities occur due to straightening the CNTs during the pre-stretching procedure.

Due to the entanglement of the CNTs in the RVE, the pre-stretch simulation prior to the embedding in the matrix involves complex contact conditions. Each CNT may interact with all other ones and contact can take place at nearly any point on the CNTs. Therefore, a highly nonlinear problem arises because of drastically changing boundary conditions. Thus, an explicit dynamic solver to perform quasi-static analyses with complex contact conditions is employed. The

general contact algorithm implemented in ABAQUS is used which detects contact between all CNTs as well as self-contact. It considers node-into-face as well as edge-to-edge penetrations and applies contact forces to prevent these. In case of contact behavior in normal direction, a "hard" contact is assumed, i.e., no contact force is applied before contact occurs and afterwards it can get infinitely high to prevent a penetration. For tangential contact behaviour, no friction is assumed as the friction coefficient of CNTs is very low (Dickrell *et al.* 2005, Cumings and Zettl 2000).

The simulation is conducted in two steps. First, the desired displacement u_{ps} is applied via a constant velocity boundary condition over a specified time span. Second, the displacement in alignment direction is fixed after the desired value is reached and oscillations due to the abrupt changes of the boundary conditions are damped until they fade out. Global mass scaling is applied to enlarge the stable time increment of the explicit integration by increasing the density. In order to ensure that the simulation is quasi-static, the energies are monitored during simulations.

3.2 Embedding CNTs in a polymer matrix

After the CNTs are stretched, they are incorporated in a polymer matrix to form a composite. Here, the embedded element technique provided by ABAQUS is utilised: elements of the CNT reinforcement are embedded within the host elements of the matrix. Evidently, the embedded and host element intersect each other. For an embedded element's node, the translational degrees of freedom are constrained by interpolated values of the host element at that position. The rotational degrees of freedom remain unconstrained.

An advantage of the employment of the embedded element technique is that the meshes of the embedded CNTs and the host matrix are generated independently of each other. A perfectly structured mesh with hexahedral C3D8R solid elements is obtained as the matrix is geometrically modelled as a cuboid. The perfectly structured mesh is automatically periodic, allowing for periodic boundary conditions. As this structured mesh does not have to resolve the microstructure, no small or distorted elements in between two close CNTs arise. Employing the embedded element technique implies perfect contact between CNTs and matrix. This assumption is admissible as in general good bonding is found in measurements of polymer-CNT interfacial shear strength (Andrews and Weisenberger 2004).

In order to incorporate deformed CNTs from the pre-stretch application into the matrix, they are imported as an orphan mesh from the end of the explicit pre-stretch simulation. At the end of the explicit simulation, stresses due to pre-stretching are saved in all integration points over the thickness of the shell elements and are subsequently applied as a pre-stress in the composite simulation.

4. Numerical examples

In the following, the experiments of Nam *et al.* (2014) are simulated to gain insight into the mechanisms behind strengthening by pre-stretching observed in these experiments. Nam *et al.* (2014) worked with CNTs (Inoue *et al.* 2008) synthesised by the group of Prof. Inoue at Shizuoka University, Japan. Hence, the characteristics of the modelled CNTs are taken from publications of that group.

The CNT diameter D is assigned randomly for each CNT based on a normal distribution with a mean value of $\mu_D = 38.1$ nm and a standard deviation of $\sigma_D = 6.6$ nm as determined by Nam *et al.*

(2015). Data to model the waviness is obtained from the analysis of micrographs published by Inoue *et al*. (2011) and Nam *et al.* (2014). In order to account for loss of information in the third dimension when analysing two-dimensional micrographs, a correction factor of $\sqrt{2}$ is used as proposed by Stein *et al.* (2015). This emulates a view angle of 45°. For the angle θ, cf. Fig. 1, a mean value of μ_θ = 5.3511° and a standard deviation of σ_θ = 5.0279° are obtained from micrographs.

Furthermore, the multi-wall CNTs are assumed to have n_w = 8 walls resulting in a thickness t = 2.72 nm of the shells used to model the CNTs. CNTs are constructed based on 21 spline points with a distance of d_s = 200 nm to each other in alignment direction, resulting in a total height of the RVE of $x_{2,\mathrm{RVE}}$ = 4 μm. The size of the RVE in transverse directions $x_{1,\mathrm{RVE}}$ and $x_{3,\mathrm{RVE}}$ is chosen in dependence of the desired volume fraction V_f. For $V_f \approx 7$ %, the RVE has a base area of 0.65 μm × 0.65 μm and for $V_f \approx 16$ %, the base area is 0.3 μm × 0.3 μm.

Jin and Yuan (2003) performed MD simulations of CNTs and discovered that they can be considered fully isotropic. Therefore, a hyperelastic isotropic material model of Neo-Hookean type is used here with the strain-energy function

$$W = \frac{\mu}{2}\left[\mathrm{I}_1(\hat{\boldsymbol{b}}) - 3\right] + \frac{\kappa}{2}[J-1]^2 \tag{1}$$

where μ is the shear modulus, I_1 the first invariant of a tensor, $\hat{\boldsymbol{b}}$ the distortional component of the left Cauchy-Green strain tensor, κ the bulk modulus and J is the determinant of the deformation gradient. Here, an elastic modulus for CNTs of E_{CNT} = 1 TPa is chosen (Lu 1997, Wong *et al.* 1997, Van Lier *et al.* 2000). Poisson's ratio is set to be ν_{CNT} = 0.28 as determined by Lu (1997) and previously used to describe CNTs synthesised by the Inoue group (Tsuda *et al.* 2014). This leads to a shear modulus μ_{CNT} = 391 GPa and a bulk modulus κ_{CNT} = 758 GPa.

For the epoxy matrix, the nonlinear hyperelastic material model of Neo-Hookean type with the strain energy function from Eq. (1) is utilised as well. The elastic properties of this epoxy have been determined in studies of the Inoue group: Ogasawara *et al.* (2011) as well as Tsuda *et al.* (2014) determined an average elastic modulus of E_{epoxy} = 2.5 GPa experimentally and, in addition, Tsuda *et al.* (2014) provide a Poisson's ratio of ν_{epoxy} = 0.3.

4.1 Effect of the matrix

In order to investigate the effect of the matrix stiffness on the CNT deformation, a simplified model is generated in which only a single wavy CNT is considered. Periodic boundary conditions are applied. Two different matrices, one with an unrealistically compliant elastic modulus of E_{unreal} = 2.5 MPa and a realistic epoxy matrix with E_{epoxy} = 2.5 GPa, are considered. For comparison, a tensile test of a single wavy CNT without a matrix is modelled as well. In this case, the displacement degrees of freedom are fixed at the bottom in all directions and at the top in transverse directions while stretching is prescribed in length direction. In all three cases, a large displacement is applied to see the effects exaggeratedly for visualisation purposes. A real composite would not be able to sustain such strains and fracture earlier.

Force-displacement curves for these three test cases are shown in Fig. 4. The curves for the single CNT and the composite with an unrealistically compliant matrix coincide almost perfectly. In the beginning, the slope is small, that is, the stiffness is low. With increased stretching, the stiffness increases up to a constant value that is the intrinsic strength of a perfectly straight CNT. A matrix with such a low stiffness seems to have no influence on the mechanical behaviour of the CNT. Contrarily, for the realistic epoxy matrix a completely different behaviour is observed. Here,

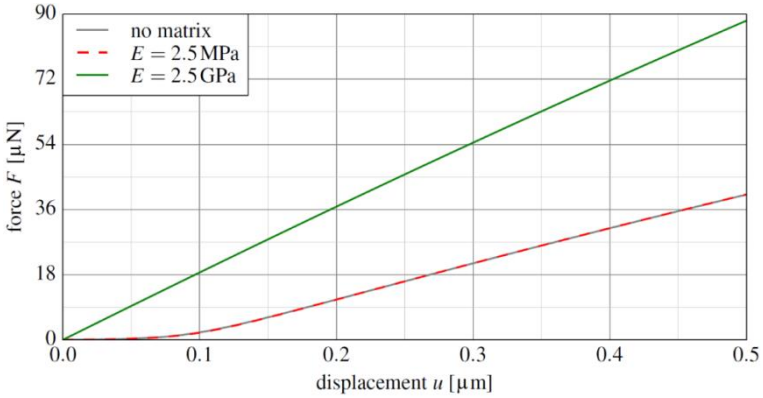

Fig. 4 Force-displacement curves of a single CNT and a single CNT embedded in matrices with different stiffnesses under tensile loading

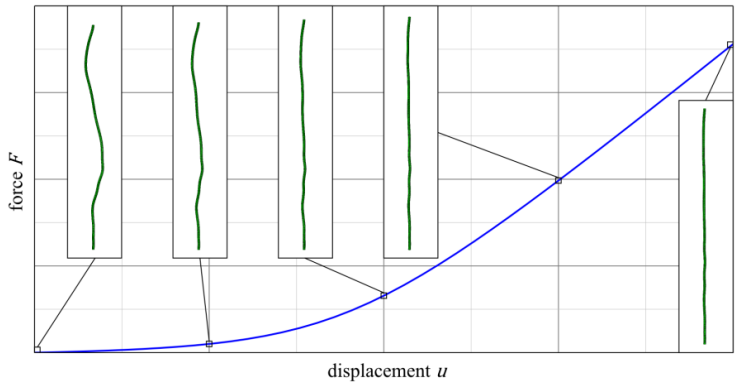

Fig. 5 Force-displacement curve of a single wavy CNT depicting the increase in stiffness during stretching due to straightening under tensile loading

almost perfectly linear elastic behaviour occurs. This is also observed in the experiments of Nam *et al.* (2014). Furthermore, the slope of the force-displacement curve is higher than that of the single CNT even if it is completely stretched. The stiffness of the matrix strongly influences to the composite behaviour and illustrates the promising properties of CNT reinforced composites.

Next, we look at the CNT's geometry during deformation. Fig. 5 illustrates the load displacement curve of a single CNT without a matrix with the corresponding deformed configurations along the curve. In the region of low stiffness, the CNT is wavy. Due to stretching, the CNT is gradually straightened, resulting in a pronounced increase in stiffness as the deformation mode of the CNT changes from bending and torsion dominated towards pure tensile loading. Evidently, the matrix affects the load transfer and, therefore, the composite's material response. In Fig. 5, the undeformed and deformed configurations of all test cases are depicted. The CNT without a matrix and the one with an unrealistically compliant matrix show the same straightening behavior (Fig. 6(a) and (b)). For the latter, the matrix is pushed to the side and does not hinder the CNT deformation. At the top and bottom of the RVE, matrix elements close to the embedded CNT are strongly distorted because of their low stiffness. A completely different behaviour is observed for the composite with the realistic matrix in Fig. 6(c). Here, the matrix

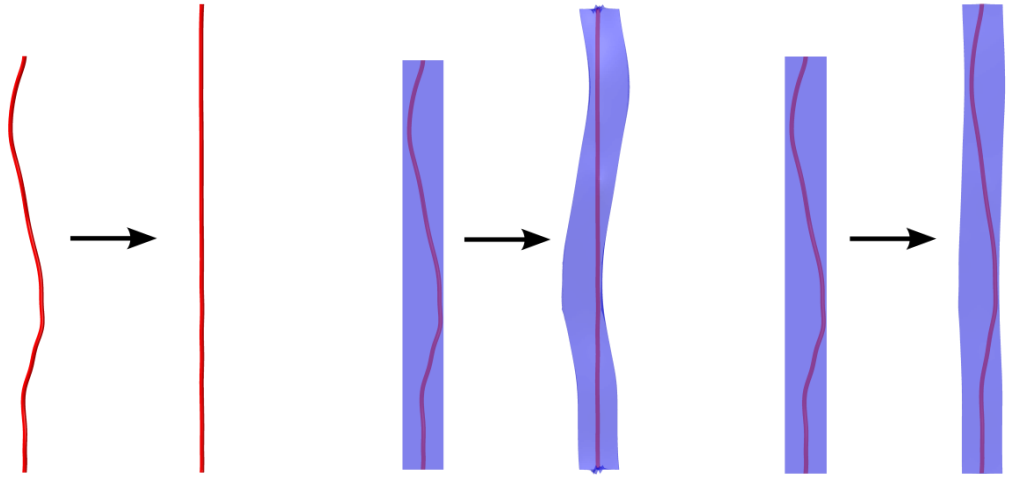

(a) No matrix (b) Unrealistically compliant matrix (c) Realistic matrix

Fig. 6 Undeformed and deformed configurations of (a) a single CNT and (b,c) a single CNT embedded in matrices with different stiffnesses under tensile loading

hinders the straightening of the CNT such that it remains wavy. Since the CNT cannot respond with a significant straightening to the applied force, its stiffness response is evidently similar to that of an already straight CNT. Thus, in case of perfect contact, a polymer as stiff as possible would be the ideal candidate for the matrix. In reality, the interface between CNTs and polymer will most probably cause larger problems for stiffer matrices, such that a trade-off between stiffness and interface conditions needs to be made.

Thus, if CNTs and matrix are in perfect contact the full potential of the mechanical properties could be used irrespective of the waviness of the CNTs. Contrarily, in reality there are problems to transfer the theoretical stiffness of CNTs to a composite due to non-perfect contact behaviour. Voids from the manufacturing process might be an explanation: the distance between CNTs in a sheet is so small that perfect infiltration by polymer resin is unlikely. In turn, this leads to shortcomings in the load transfer between CNTs and matrix. Furthermore, the interfacial shear strength and load transfer between CNT and polymer could be problematic (Goh *et al.* 2014). The perfect atomic structure of CNTs results in smooth surfaces and therefore reduces the efficiency of the load transfer between matrix and reinforcement. To counteract these effects that are difficult to overcome, Nam *et al.* (2014) suggest the possibility of pre-stretching CNT sheets before embedding in the polymer. The effect of such a pre-stretching is studied in the following.

4.2 Effect of pre-stretching

To investigate the effect of pre-stretching of CNTs before embedding them in the matrix, pre-stretches of $\varepsilon_{ps} = 0.02$ and $\varepsilon_{ps} = 0.03$ for the pure CNT sheets are modelled in accordance with experiments of Nam *et al.* (2014). Higher pre-stretches such as $\varepsilon_{ps} = 0.04$ are not investigated because these lead to sliding within CNT sheets in experiments due to van der Waals forces. The simulation results are then compared with the experiments of Nam *et al.* (2014) to investigate the potential of pre-stretching in transferring the outstanding theoretical mechanical properties of CNTs to composites.

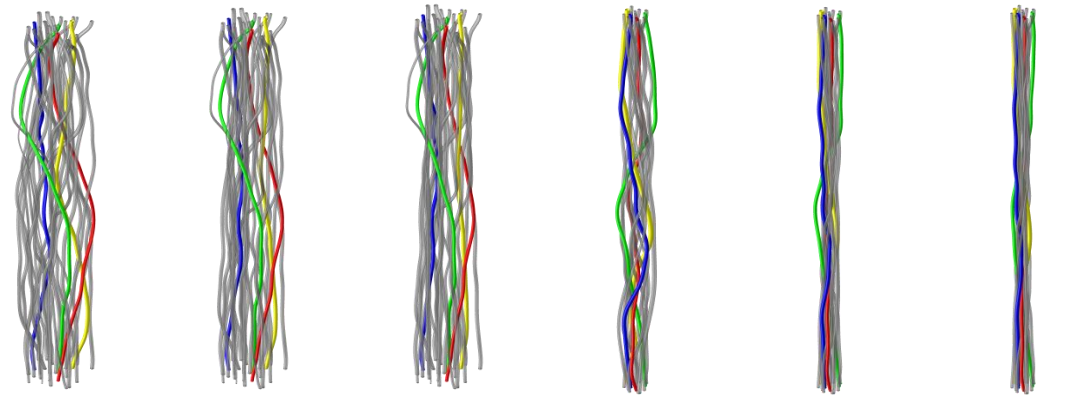

$\varepsilon_{ps} = 0.00$ $\varepsilon_{ps} = 0.02$ $\varepsilon_{ps} = 0.03$ $\varepsilon_{ps} = 0.00$ $\varepsilon_{ps} = 0.02$ $\varepsilon_{ps} = 0.03$

(a) Volume fraction of $V_f \approx 7$ % (b) Volume fraction of $V_f \approx 16$ %

Fig. 7 Straightening of wavy CNTs during pre-stretching of CNT sheets corresponding to RVEs with a volume fraction of $V_f \approx 7$ % and $V_f \approx 16$ %. Arbitrary CNTs are highlighted by colours in order to visualise the deformation behaviour

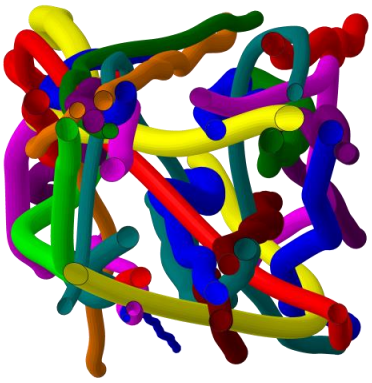

Fig. 8 Cut through a pre-stretched CNT sheet showing regions in which several CNTs are twisted and wound around each other, forming dense bundles

CNT sheet RVEs that correspond to composites with a volume fraction of $V_f \approx 7$ % and $V_f \approx 16$ % are displayed in Fig. 7 under different amounts of pre-stretch. Due to the pre-stretch, the waviness is considerably reduced for $V_f \approx 7$ % as seen in Fig. 7(a). Nevertheless, some of the CNTs still remain relatively wavy. Furthermore, a twisting and winding of CNTs around each other in the middle of the sheet is visible, see Fig. 3. These two effects lead to a more slender sheet. For $V_f \approx 16$ %, a pre-stretch significantly reduces the waviness as well, as seen in Fig. 7(b). In contrast to Fig. 7(a), there is almost no CNT that still exhibits higher waviness. Except for twisting and winding in the middle of the sheet, all CNTs are almost straight. In addition, slimming of the sheet is observed. This leads to an increase in volume fraction and is even more distinct than for the lower volume fraction CNT sheet RVE.

Several CNTs cluster together as bundles and form ropes inside the sheet as also observed in experiments (Nam *et al.* 2014). This is visible in the cut through a pre-stretched CNT sheet presented in Fig. 8. It also depicts the complexity of the contact boundary conditions arising from

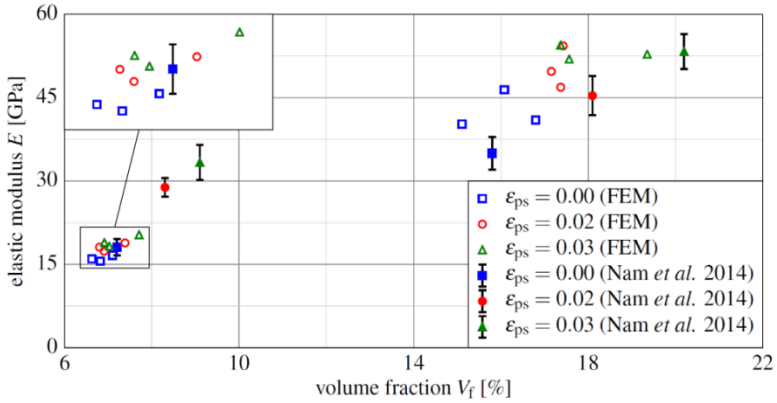

Fig. 9 Comparison of influence of pre-stretch ε_{ps} on effective elastic modulus E of the composite for experiments of Nam *et al.* (2014) and FEM simulations

the deformation. An individual CNT can be in contact with several other ones and the twisting can lead to a spiral like line contact around the circumference of the CNT.

The pre-stretched CNT sheet RVEs are then embedded in an epoxy matrix as described in Section 3.2. To account for the slimming of the sheet and the resulting increase in volume fraction, the dimensions of the cuboid matrix are chosen to be only slightly larger than the outermost points of the deformed sheet.

Tensile test simulations of the composite RVEs including pre-stretched CNTs are carried out with a maximum strain of $\varepsilon = 0.005$ to determine the composite's effective stiffness. For larger strains, fracture occurred in the experiments of Nam *et al.* (2014). The simulated stress response to an applied strain is used to determine the effective elastic modulus from a least squares fit of Hooke's law.

For both volume fractions of $V_f \approx 7$ % and $V_f \approx 16$ %, three RVEs are analysed. An unstretched and two pre-stretched CNT sheets with $\varepsilon_{ps} = 0.02$ and $\varepsilon_{ps} = 0.03$ are considered as reinforcements. A comparison of FEM simulations and experiments of Nam *et al.* (2014) in terms of the effective elastic modulus E of the composite under the influence of pre-stretch ε_{ps} is shown in Fig. 9. The simulation results are in very good agreement with experiments and show an increase in stiffness of about 30 % in response to a 3 % pre-stretch for higher volume fraction. For lower volume fraction, the increase in stiffness of the RVEs is not as pronounced. Without pre-stretch, the lower volume fraction RVEs are slightly more compliant than the experiments while the higher volume fraction RVEs behave a little stiffer. One possible explanation for this discrepancy lies in the waviness of CNTs which in the following is quantified by the tortuosity τ

$$\tau = \frac{l_{\mathrm{CNT}}}{h_{\mathrm{RVE}}}. \tag{2}$$

The tortuosity relates the arc length l_{CNT} of an indivual CNT to its projected length in alignement direction, which in case of the considered endless CNTs is given by the height of the RVE h_{RVE}.

In Fig. 10(a), the effective elastic modulus E of the composite is displayed in dependence of the tortuosity τ. The tortuosity is considerably higher for lower volume fraction RVEs. From experiments (Yu *et al.* 2000) it is known that for straight multi-wall CNTs under tension, almost

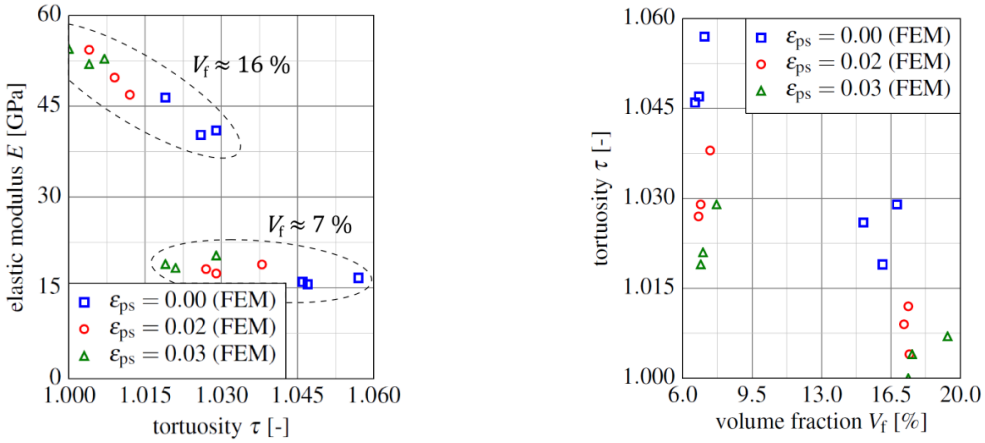

(a) Influence of tortuosity τ on elastic modulus E (b) Influence of pre-stretch ε_{ps} on tortuosity τ

Fig. 10 Effective elastic modulus E of the composite under influence of tortuosity τ and its own dependence on pre-stretch ε_{ps}

the whole load is carried by the outermost layer as the interlayer shear strength is small. Contrarily, for bending deformation, all walls are "active" and carry load (Ru 2000). Tensile loading of a wavy CNT is a combination of tension and bending deformation. With increasing tortuosity of the CNTs, bending becomes the dominant deformation mode. Thus, for the lower volume fraction RVEs with higher tortuosity, more walls are "active" and the choice of $n_w = 8$ might be smaller than in reality. In contrast, for the higher volume fraction RVEs with lower tortuosity, less walls are "active" and the choice of $n_w = 8$ might be too high. The number of "active" walls is not captured by the proposed model as all walls are modelled with a single shell layer. The walls would need to be modelled individually to account for this effect. Here, $n_w = 8$ is used since this results in reasonable deviations for both volume fraction RVEs. However, a refined model could give further insight into the phenomenon.

5. Conclusions

A procedure to generate RVEs that accurately model the microstructure of an aligned CNT sheet embedded into a polymer matrix is presented. The RVEs generated with the presented technique are the first to exhibit realistically high volume fractions while also accounting for random waviness and intertwining of CNTs. Waviness, entanglement and intertwining are accounted for by introducing randomness into the geometry generation. The parameters characterising the waviness are obtained from micrographs of CNT sheets. The randomly wavy geometry of an individual CNT is described by a sweep of a circle along a cubic spline. Thus, the high continuity of CNTs is captured and artificial stress concentrations at kinks are avoided that arise in other modelling approaches based on sequences of straight line segments. Modelling multi-walled CNTs as a single layer of shell elements yields a very good compromise between representation accuracy and computational time.

Our RVEs are naturally periodic and capture high volume fractions of CNTs without resulting in excessively fine or distorted meshes. We study the material behaviour of aligned CNT sheets as

well as embedment into a matrix to investigate composites.

Numerical studies of pre-stretching CNT sheets before inclusion in a polymeric matrix are carried out using the proposed RVE. Due to the realistic representation of the wavy, entangled geometry of CNT, our analysis gives valuable insight into how different influencing factors such as matrix properties, volume fraction and waviness interact and evolve during the process and how they affect the composite's effective mechanical properties. Pre-stretching is shown to significantly reduce the waviness of the reinforcing CNTs and to increase the stiffness of the composite. The qualitative and quantitative information gained from numerical studies based on RVEs as detailed as the proposed one helps in developing methods to transfer the outstanding mechanical properties of individual CNTs to composite materials.

Acknowledgments

Financial support from the German Research Foundation (DFG) via SFB 986 "M3" (project B6) is gratefully acknowledged. The authors thank Prof. Norbert Huber at Helmholtz-Zentrum Geesthacht for helpful discussions.

References

Andrews, R. and Weisenberger, M.C. (2004), "Carbon nanotube polymer composites", *Curr. Opin. Sol. State Mater. Sci.*, **8**(1), 31-37.

Bradshaw, R.D., Fisher, F.T. and Brinson, L.C. (2003), "Fiber waviness in nanotube-reinforced polymer composites-II: Modeling via numerical approximation of the dilute strain concentration tensor", *Compos. Sci. Technol.*, **63**(11), 1705-1722.

Cheng, H.C., Liu, Y.L., Hsu, Y.C. and Chen, W.H. (2009), "Atomistic-continuum modeling for mechanical properties of single-walled carbon nanotubes", *J. Sol. Struct.*, **46**(7), 1695-1704.

Cumings, J. and Zettl, A. (2000), "Low-friction nanoscale linear bearing realized from multiwall carbon nanotubes", *Sci.*, **289**(5479), 602-604.

Dastgerdi, J.N., Marquis, G. and Salimi, M. (2013), "The effect of nanotubes waviness on mechanical properties of CNT/SMP composites", *Compos. Sci. Technol.*, **86**, 164-169.

Demczyk, B.G., Wang, Y.M., Cumings, J., Hetman, M., Han, W., Zettl, A. and Ritchie, R.O. (2002), "Direct mechanical measurement of the tensile strength and elastic modulus of multiwalled carbon nanotubes", *Mater. Sci. Eng.: A*, **334**(1), 173-178.

Dickrell, P.L., Sinnott, S.B., Hahn, D.W., Raravikar, N.R., Schadler, L.S., Ajayan, P.M. and Sawyer, W.G. (2005), "Frictional anisotropy of oriented carbon nanotube surfaces", *Tribol. Lett.*, **18**(1), 59-62.

Fisher, F.T., Bradshaw, R.D. and Brinson, L.C. (2002), "Effects of nanotube waviness on the modulus of nanotube-reinforced polymers", *Appl. Phys. Lett.*, **80**(24), 4647-4649.

Fisher, F.T., Bradshaw, R.D. and Brinson, L.C. (2003), "Fiber waviness in nanotube-reinforced polymer composites-I: Modulus predictions using effective nanotube properties", *Compos. Sci. Technol.*, **63**(11), 1689-1703.

Ginga, N.J., Chen, W. and Sitaraman, S.K. (2014), "Waviness reduces effective modulus of carbon nanotube forests by several orders of magnitude", *Carbon*, **66**, 57-66.

Goh, P.S., Ismail, A.F. and Ng, B.C. (2014), "Directional alignment of carbon nanotubes in polymer matrices: Contemporary approaches and future advances", *Compos. Part A*, **56**, 103-126.

Govindjee, S. and Sackman, J.L. (1999), "On the use of continuum mechanics to estimate the properties of nanotubes", *Sol. State Commun.*, **110**(4), 227-230.

Grady, B.P. (2011), *Carbon Nanotube-Polymer Composites: Manufacture, Properties, and Applications*, John Wiley & Sons, New York, U.S.A.

Herasati, S. and Zhang, L. (2014), "A new method for characterizing and modeling the waviness and alignment of carbon nanotubes in composites", *Compos. Sci. Technol.*, **100**, 136-142.

Hernández, E., Goze, C., Bernier, P. and Rubio, A. (1998), "Elastic properties of C and $B_xC_yN_z$ composite nanotubes", *Phys. Rev. Lett.*, **80**(20), 4502.

Iijima, S. (1991), "Helical microtubules of graphitic carbon", *Nat.*, **354**(6348), 56-58.

Inoue, Y., Kakihata, K., Hirono, Y., Horie, T., Ishida, A. and Mimura, H. (2008), "One-step grown aligned bulk carbon nanotubes by chloride mediated chemical vapor deposition", *Appl. Phys. Lett.*, **92**(21), 213113.

Inoue, Y., Suzuki, Y., Minami, Y., Muramatsu, J., Shimamura, Y., Suzuki, K., Ghemes, A., Okada, M., Sakakibara, S., Mimura, H. and Naito, K. (2011), "Anisotropic carbon nanotube papers fabricated from multiwalled carbon nanotube webs", *Carbon*, **49**(7), 2437-2443.

Jin, Y. and Yuan, F.G. (2003), "Simulation of elastic properties of single-walled carbon nanotubes", *Compos. Sci. Technol.*, **63**(11), 1507-1515.

Kassem, G. (2010), "Micromechanical material models for polymer composites through advanced numerical simulation techniques", Ph.D. Dissertation.

Kouznetsova, V.G., Geers, M.G.D. and Brekelmans, W.A.M. (2010), "Computational homogenization for non-linear heterogeneous solids", *Multisc. Model. Sol. Mech.*: *Comput. Appro.*, 1-42.

Li, C. and Chou, T.W. (2003), "A structural mechanics approach for the analysis of carbon nanotubes", *J. Sol. Struct.*, **40**(10), 2487-2499.

Lu, J.P. (1997), "Elastic properties of carbon nanotubes and nanoropes", *Phys. Rev. Lett.*, **79**(7), 1297.

Mecklenburg, M., Mizushima, D., Ohtake, N., Bauhofer, W., Fiedler, B. and Schulte, K. (2015), "On the manufacturing and electrical and mechanical properties of ultra-high wt.% fraction aligned MWCNT and randomly oriented CNT epoxy composites", *Carbon*, **91**, 275-290.

Nam, T.H., Goto, K., Nakayama, H., Oshima, K., Premalal, V., Shimamura, Y, Inoue, Y., Naito, K. and Kobayashi, S. (2014), "Effects of stretching on mechanical properties of aligned multi-walled carbon-nanotube/epoxy composites", *Compos. Part A*, **64**, 197-202.

Nam, T.H., Goto, K., Yamaguchi, Y., Premalal, E., Shimamura, Y., Inoue, Y., Naito, K. and Ogihara, S. (2015), "Effects of CNT diameter on mechanical properties of aligned CNT sheets and composites", *Compos. Part A*, **76**, 289-298.

Paunikar, S. and Kumar, S. (2014), "Effect of CNT waviness on the effective mechanical properties of long and short CNT reinforced composites", *Comput. Mater. Sci.*, **95**, 21-28.

Ru, C.Q. (2000), "Effective bending stiffness of carbon nanotubes", *Phys. Rev. B*, **62**(15), 9973.

Salvetat, J.P., Kulik, A.J., Bonard, J.M., Briggs, G.A.D., Stöckli, T., Méténier, K., Bonnamy, S., Béguin, F., Burnham, N.A. and Forró, L. (1999), "Elastic modulus of ordered and disordered multiwalled carbon nanotubes", *Adv. Mater.*, **11**(2), 161-165.

Schneider, K., Klusemann, B. and Bargmann, S. (2016), "Automatic three-dimensional geometry and mesh generation of periodic representative volume elements for matrix-inclusion composites", *Adv. Eng. Soft.*, **99**, 177-188.

Schneider, K., Klusemann, B. and Bargmann, S. (2017), "Fully periodic RVEs for technological relevant composites: Not worth the effort!", *J. Mech. Mater. Struct.*, In press.

Shady, E. and Gowayed, Y. (2010), "Effect of nanotube geometry on the elastic properties of nanocomposites", *Compos. Sci. Technol.*, **70**(10), 1476-1481.

Shi, D.L., Feng, X.Q., Huang, Y.Y., Hwang, K.C. and Gao, H. (2004) "The effect of nanotube waviness and agglomeration on the elastic property of carbon nanotube-reinforced composites", *J. Eng. Mater. Technol.*, **126**, 250-257.

Stein, I.Y., Lewis, D.J. and Wardle, B.L. (2015), "Aligned carbon nanotube array stiffness from stochastic three-dimensional morphology", *Nanos.*, **7**(46), 19426-19431.

Thostenson, E.T., Li, C. and Chou, T.W. (2005), "Nanocomposites in context", *Compos. Sci. Technol.*, **65**(3), 491-516.

Tsuda, T., Ogasawara, T., Moon, S.Y., Nakamoto, K., Takeda, N., Shimamura, Y. and Inoue, Y. (2014), "Three dimensional orientation angle distribution counting and calculation for the mechanical properties of aligned carbon nanotube/epoxy composites", *Compos. Part A*, **65**, 1-9.

Van Lier, G., Van Alsenoy, C., Van Doren, V. and Geerlings, P. (2000), "Ab initio study of the elastic properties of single-walled carbon nanotubes and graphene", *Chem. Phys. Lett.*, **326**(1), 181-185.

Wernik, J.M. and Meguid, S.A. (2010), "Atomistic-based continuum modeling of the nonlinear behavior of carbon nanotubes", *Acta Mech.*, **212**(1), 167-179.

Wong, E.W., Sheehan, P.E. and Lieber, C.M. (1997), "Nanobeam mechanics: Elasticity, strength, and toughness of nanorods and nanotubes", *Sci.*, **277**(5334), 1971-1975.

Yakobson, B.I. and Smalley, R.E. (1997), "Fullerene nanotubes: $C_{1,000,000}$ and beyond", *Am. Sci.*, **85**(4), 324-337.

Yu, M.F., Lourie, O., Dyer, M.J., Moloni, K., Kelly, T.F. and Ruoff, R.S. (2000), "Strength and breaking mechanism of multiwalled carbon nanotubes under tensile load", *Sci.*, **287**(5453), 637-640.

Yuan, Z. and Fish, J. (2008), "Computational homogenization in practice", *J. Numer. Meth.* Eng., **73**(3), 361-380.

DC